ChemComm

COMMUNICATION

View Article Online
View Journal | View Issue

Cite this: *Chem. Commun.*, 2021, **57**, 4291

Received 10th February 2021,
Accepted 24th March 2021

DOI: 10.1039/d1cc00791b

rsc.li/chemcomm

Assessing multiple conformations of lanthanide binding tags for proteins using a sensitive ^{19}F-reporter†

Jia-Liang Chen, Ben-Guang Chen, Bin Li, Feng Yang and Xun-Cheng Su *

Quantifying the isomeric species of metal complexes in solution is difficult. ^{19}F NMR herein was used to determine the abundance of isomeric species and dynamic properties of lanthanide binding tags. The results suggest that ^{19}F is an efficient reporter in assessing and screening paramagnetic tags suitable for protein NMR analysis.

Relying on the dipolar interactions between the unpaired electron and nuclei spins in biomolecules or ligands, paramagnetic effects manifested in NMR spectroscopy have been widely used in characterizing the structures and dynamics of proteins and protein complexes, nucleotides, and oligosaccharides.[1,2] To achieve these rich sources of structural restraints, site-specific labeling of proteins with a paramagnetic tag is generally required. Lanthanide ions (Ln^{3+}) are preferred in the generation of long-range distance and angular restraints of biomolecules in structural biology,[1] and chemically synthesized lanthanide binding tags represent a mainstream in site-specific labeling of proteins with a paramagnetic tag.[3]

Because of the magnetic anisotropy and high coordinating numbers of lanthanide ions, multiple paramagnetic species are generally present in the protein–tag conjugates as evidenced in the high resolution NMR spectra. It is indeed in the following cases, if the tag generates a new chiral center once attached to a protein[4a] or the coordination core of metal complexes contains a chiral center[4b–d] or multiple conformation states in slow exchange in the NMR timescale.[5] In contrast, only one diamagnetic species is generally observed in the protein–tag conjugates. Therefore, the chirality has to be carefully considered in the design of suitable paramagnetic tags for applications in biological systems. However, elucidation of multiple paramagnetic species in the paramagnetic tags is difficult by proton based NMR spectra, because the chemical shift assignments of the individual protons are complex and difficult due to the chemical exchange broadening and the large paramagnetic shift and paramagnetic relaxation enhancement nearby the paramagnetic center.[6] Here, we used ^{19}F-NMR to discriminate the different conformations of paramagnetic species.

The lanthanide (Ln) complexes of 1,4,7,10-tetraazacyclododecane-*N*,*N*′,*N*″,*N*‴-tetraacetic acid (DOTA) and its derivatives are kinetically inert but show a diverse range in the magnetic anisotropy, and these complexes are widely used in paramagnetic NMR of proteins.[3] DOTA–Ln complexes generally present two main isomeric states (four enantiomeric pairs), the square antiprism (SAP) and twisted square antiprism (TSAP) conformations, in solution due to the ring inversion and arm rotation.[7] The abundance of the two isomers highly depends on the ionic radius of Ln^{3+}.[7] These two isomers differ greatly in water exchange rates and magnetic anisotropy.[8] The difficulty in using DOTA–Ln complexes as paramagnetic tags in structural biology is the ease of forming multiple paramagnetic species in solution.[3,5b–e] To achieve a guideline in designing suitable DOTA–Ln like tags for applications in biological systems, we used ^{19}F NMR to quantify the isomer populations in the free DOTA–Ln like tag and testify this concept in the protein–tag conjugates.

We synthesized two DOTA–Ln like tags, 4PS-5F-Py-DO3MA(S)-Ln (T1-Ln) and 4PS-5F-Py-DO3A-Ln (T2-Ln) (Ln = Lu, Yb, Tm, Tb, Dy) following the previous protocol with some modifications (Fig. 1) (detail in the ESI†).[9] Each tag contains a thiol reactive phenylsulfone group (PS) at the fourth position in pyridine, which can be conjugated to a solvent cysteine in a protein.[10] To reduce

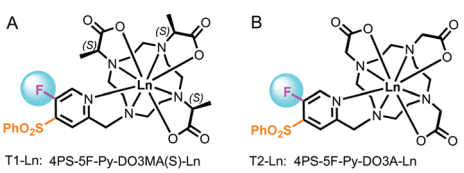

Fig. 1 Chemical structures of DOTA derived paramagnetic tags, 4PS-5F-Py-DO3MA(S)-Ln (A), and 4PS-5F-Py-DO3A-Ln (B). Each tag contains a thiol-specific reaction moiety, phenylsulfonated pyridine (ref. 9 and 10), and a ^{19}F NMR reporter.

State Key Laboratory of Elemento-organic Chemistry, College of Chemistry, Nankai University, Tianjin 300071, China. E-mail: xunchengsu@nankai.edu.cn

† Electronic supplementary information (ESI) available. See DOI: 10.1039/d1cc00791b

the paramagnetic relaxation enhancement effect, one fluorine was anchored at the 5-position of the pyridine ring, which is distant from the paramagnetic center (Fig. 1). The two tags were assessed by 1D ^{19}F NMR, and the isomeric exchange rates were extracted by 2D ^{19}F-EXSY spectra.

In the 1D ^{19}F NMR spectra, one single ^{19}F signal was observed for the T1-Lu and T1-Yb complexes (Fig. 2A). In contrast, two sets of ^{19}F signals in varied populations were determined for the T1 complexes with Tm^{3+}, Tb^{3+} and Dy^{3+}. The abundance of minor species was about 10%, 18%, and 15% for Tm^{3+}, Dy^{3+}, and Tb^{3+} complexes, respectively (Table 1). Different from T1-Ln, both diamagnetic and paramagnetic complexes of T2-Ln presented two species in solution (Fig. 2B). The minor species in T2-Ln complexes was about 25%, 22%, 15%, 10%, and 18% for Lu^{3+}, Yb^{3+}, Tm^{3+}, Dy^{3+}, and Tb^{3+}, respectively (Table 1). To characterize the dynamic exchange properties between the two isomeric species, 2D ^{19}F-EXSY experiments were performed (Fig. S2 and S3, ESI†). Notably, the chemical shift difference between two isomeric species increased from about 2 ppm to tens of ppm (Table 1). The reaction product of L-cysteine with tag–Ln complexes (Ln = Lu, Yb, Tm) preserves similar populations for the two isomers in solution (Fig. S4 and Table S1, ESI†), indicating that the phenylsulfone group in the pyridine has no significant effect on the isomeric diversity. These data suggest that the 1D and 2D ^{19}F-NMR spectra are efficient to discriminate and quantify the isomeric species of DOTA–Ln like complexes in solution. The EXSY data showed a minor species with a population of about 5% and 4% for T1-Yb and T1-Lu complexes that was not visible in the 1D NMR spectrum of the 1.0 mM complex (Fig. 2 and Fig. S5, ESI†).

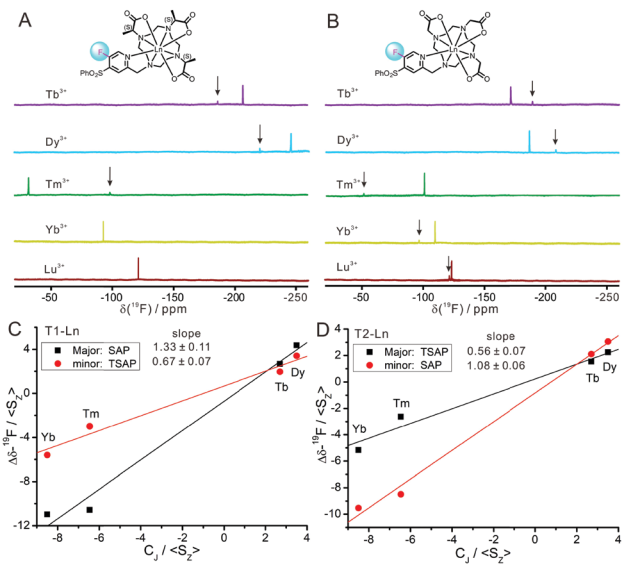

Fig. 2 1D ^{19}F NMR spectra of the T1-Ln (A) and T2-Ln (B) (Ln = Lu, Yb, Tm, Dy, Tb) complexes. The arrow denotes the minor species. The Reilley plot of $\Delta\delta$-^{19}F/$\langle S_Z\rangle$ *vs.* $C_J/\langle S_Z\rangle$ was performed for the major (black) and minor (red) species in T1-Ln (C) and T2-Ln complexes (D). $\Delta\delta$-^{19}F is the chemical shift difference between the paramagnetic species and diamagnetic species. Experimental details are in the ESI† and the values of C_J and $\langle S_Z\rangle$ for Ln^{3+} are from ref. 12.

Table 1 ^{19}F chemical shifts and populations (*P*) of the two isomers in T1-Ln and T2-Ln complexes determined by 1D ^{19}F NMR spectra, and $\Delta\delta^{AB}$ is the absolute value of the chemical shift differences between the two isomeric species

	Isomer A (SAP)			Isomer B (TSAP)		
	Ln	δ (ppm)	*P* (%)	δ (ppm)	*P* (%)	$\Delta\delta^{AB}$
T1-Ln	Lu	−121.38	96	−123.60	4[a]	2.22
	Yb	−92.99	95	−108.70	5[a]	15.71
	Tm	−34.60	90	−98.65	10	64.05
	Dy	−246.06	82	−220.65	18	25.41
	Tb	−206.56	85	−186.05	15	20.51
T2-Ln	Lu	−121.41	25	−123.16	75	1.75
	Yb	−96.76	22	−109.78	78	13.02
	Tm	−51.68	15	−101.56	85	49.88
	Dy	−208.55	10	−187.00	90	21.55
	Tb	−188.23	18	−172.00	82	16.23

[a] The minor species in T1-Lu and T1-Yb was determined by an EXSY experiment.

In the T1-Ln complexes, the major species has larger lanthanide induced shifts (LIS) than the minor one, whereas T2-Ln complexes present an opposite trend (Fig. 2 and Fig. S6, ESI†). The different isomers for the major species between the T1-Ln and T2-Ln complexes is due to the effect of the additional methyl group in the arm. In the DOTA–Ln complexes, the SAP isomer adopts a large torsion angle between the N_4 and O_4 planes ($\sim 39^\circ$) and a more compact coordinating cage than the TSAP isomer.[7] The SAP isomer presents a stronger ligand field than the TSAP isomer.[8c,11] The ligand field parameters can be determined by Reilley analysis of LIS,[12] and the contact (δ_C) and pseudocontact (δ_{PCS}) terms under the axial symmetry assumption can be written as

$$\delta_{PCS} = \Delta\chi_{ax}\left(\frac{3\cos^2\theta - 1}{12\pi r^3}\right) = \frac{\mu_0{\mu_B}^2 C_J B_2^0}{10(kT)^2}\left(\frac{3\cos^2\theta - 1}{12\pi r^3}\right) \quad (1)$$

$$\mathrm{LIS} = \delta_{para} - \delta_{dia} = \delta_C + \delta_{PCS} = \langle S_Z\rangle F + C_J G \quad (2)$$

$$\frac{\mathrm{LIS}}{\langle S_Z\rangle} = F + \frac{C_J}{\langle S_Z\rangle}G \quad (3)$$

where $\Delta\chi_{ax}$ is the axial component of the magnetic susceptibility tensor, r and θ are polar coordinates of the nucleus relative to the anisotropic $\Delta\chi$-tensors, μ_0 is the permeability of vacuum, μ_B is the Bohr magneton, B_2^0 is the second rank ligand field parameter. $\langle S_Z\rangle$ and C_J are lanthanide-dependent constants, F is the observed nucleus dependent value, and G is the value dependent on the ligand field parameters and the geometric location of the observed nucleus.[12] As shown in eqn (3), the plot of LIS/$\langle S_Z\rangle$ with respect to $C_J/\langle S_Z\rangle$ generates a linear relationship and the slope represents the strength of the ligand field.

The major species of T1-Ln complexes presents a larger slope than the minor species from the Reilley plot according to eqn (3) (1.33 for major species and 0.67 for minor species) (Fig. 2C), suggesting that the major species adopts the SAP state and the minor species is in the TSAP state. This result is consistent with the previous observations in LnDOTA,[13a]

LnDO3A-SA,[13b] and LnNB-DOTA.[13c] In contrast, the major species of T2-Ln complexes is in the TSAP state, since its slope (0.56) is smaller than that of the minor species (1.08) from the Reilley plot (Fig. 2D). The population of isomeric species in T2-Ln complexes is similar to those in the LnHPDO3A[11d] and LnDOTMA(R).[13d] We note that T2-Ln (Ln = Tb, Dy, Tm, Yb, and Lu) complexes differ from the PyDO3A-Eu, which has 66% SAP state.[13e] This is probably due to the variations in the ion radius.[5e,7,11d] To summarize, the LIS plot of the ^{19}F nucleus is an efficient reporter to determine the individual isomers of DOTA–Ln like complexes in solution.

The inspiring results demonstrated by ^{19}F-NMR encouraged us to determine the isomeric exchange rates in solution, which is highly important for site-specific tagging proteins.[5f] We performed EXSY experiments for the T1-Yb and T2-Yb complexes with mixing time varying from 1 ms to 30 ms to extract isomeric exchange parameters (details in the ESI†).[7b,14] As shown in Fig. 3, the fitted exchange rate between the two isomers was 165 ± 13 s^{-1} for the T1-Yb complex. The abundance of the TSAP and SAP states is 96% and 4%, respectively, which was not identified by 1D ^{19}F NMR (Fig. 2A and Table 1). Similarly, the fitted exchange rate between the two isomers is 276 ± 16 s^{-1} for the T2-Yb complex, which is faster than that of the T1-Yb complex (Fig. 3) because of the absence of the methyl group in the arm. The relative population was 76% in the TSAP state and 24% in the SAP state, consistent with the results of 1D ^{19}F NMR. Interestingly, a third conformation (about 1%) was also observed in the 2D ^{19}F-EXSY spectra of the T2-Yb complex, and this additional isomer was readily transformed to the SAP rather than the TSAP isomer and the exchange rate was 131 ± 1 s^{-1} (Fig. 3). The value is similar to the arm-rotation rate but larger than the ring-inversion rates in the DOTA–Ln like complexes,[13b,14] indicating that the third isomer in the T2-Yb complex might stem from the 4PS-pyridine arm rotation as found in LnDO3A-SA[13b] and some DO3A-Ln like complexes.[11d,15] To summarize, the T1-Ln complexes have higher conformational stability than T2-Ln complexes due to the introduction of a methyl group at the coordination arms.[14c]

To evaluate whether the isomeric species in the free tag is held true in its protein conjugates, we used human ubiquitin G47C as a target protein to assess these two tags. In the G47C-T1-Ln (Ln = Tm, Yb) conjugates, one major paramagnetic species with large PCSs was observed in the 2D ^{15}N-HSQC spectra (Fig. 4 and Fig. S7, ESI†). A minor paramagnetic species with population of 12% ± 3% for G47C-T1-Tm and 5.4% ± 1.5% for the G47C-T1-Yb conjugate were also observed, consistent with the results of free T1-Ln complexes (Fig. 4, Table 1 and Fig. S7, ESI†). The 1D ^{19}F NMR of G47C-T1-Tm presented a similar result (Fig. 4). In addition, the G47C-T1-Tm conjugate showed strikingly different PCSs from the G47C-PyDO3MA(S)-Tm conjugate (Table S2 and Fig. S8, S9, ESI†),[16] indicating that the fluorine atom tunes the relative orientation of the tag–Ln complex to protein. In great contrast, two sets of paramagnetic species with different PCSs were observed in the G47C-T2-Ln (Ln = Tm, Yb) conjugates (Fig. 4 and Fig. S7, ESI†). The two paramagnetic species have similar populations of 48% ± 2%, and 52% ± 2% in the G47C-T2-Tm conjugate and 44% ± 2.5%, and 56% ± 2.5% in the G47C-T2-Yb conjugate, respectively, strikingly different from the free T2-Ln complexes (Table 1, Fig. 4 and Fig. S7, ESI†). The 1D ^{19}F NMR of the G47C-T2-Tm conjugate had a similar but slightly skewed result due to the broad signals in the minor species (Fig. 4). The inconsistency between the free T1-Ln and T2-Ln tags and the protein conjugates suggests the impact of the local environment surrounding the ligation site on the conformational stability and isomeric interconversion of the tag–Ln complex, especially for the dynamic-lability DO3A-Ln like tag (Fig. 4 and Fig. S7, ESI†). The decreased isomeric exchange rate by the

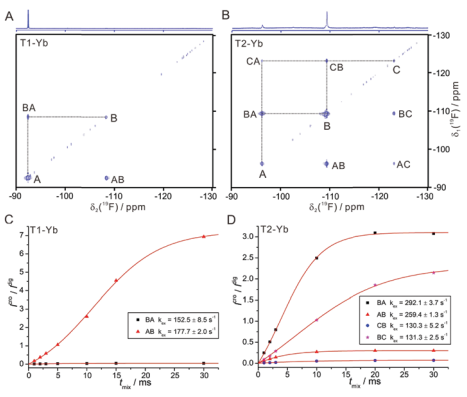

Fig. 3 Exchange rates between different isomers determined by 2D ^{19}F-EXSY spectra for the DOTA–Ln complexes. The ^{19}F-EXSY spectra: (A) T1-Yb, and (B) T2-Yb. The exchange rates between different isomers: (C) T1-Yb, and (D) T2-Yb. The NMR spectra were recorded for the 20 mM lanthanide complex with a mixing time of 20 ms.

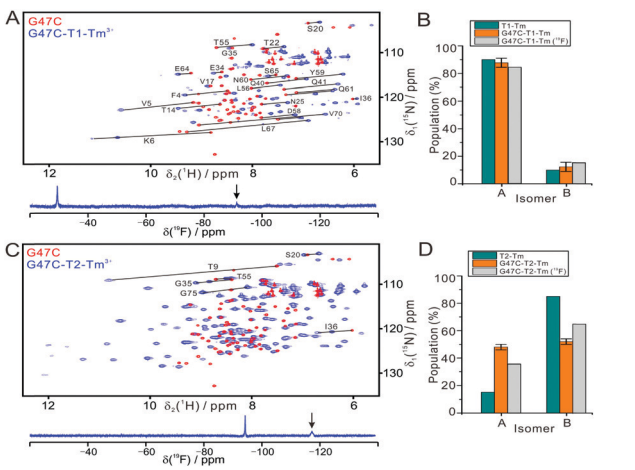

Fig. 4 Isomeric species of two DOTA–Ln like complexes evaluated in ubiquitin G47C conjugates. 1D ^{19}F NMR and ^{15}N-HSQC spectra overlay of 0.2 mM Ub G47C-Tag–Tm conjugate (blue) and 0.2 mM Ub G47C (red) recorded in 20 mM MES buffer at pH 6.4 and 298 K for (A) T1-Tm and (C) T2-Tm, respectively. The arrow denotes the minor species. Comparison of populations of two isomers in free tag–Tm (cyan) and Ub G47C-Tag–Tm conjugate (^{15}N-HSQC: orange, ^{19}F NMR: gray) for (B) T1-Tm and (D) T2-Tm, respectively.

introduction of a substitution group in the DOTA-like tags is more favorable to preserve the isomeric state in the protein conjugates. The results are similar to the previously reported L-Cys-DTPA tag,[5f] suggesting that the dynamic exchange of the tag–Ln complex is an important factor in defining the rigidity of the protein-tag conjugate. Therefore, the isomeric exchange rate that is not achieved by HPLC, mass spectra and CD spectra, is an important issue to be considered for applications of biological systems by NMR.

To summarize, we show herein that ^{19}F is a sensitive reporter in delineating and quantifying the isomers of lanthanide binding complexes in solution without awkward assignments in the routine ^{1}H NMR. Combining the paramagnetic shift analysis, ^{19}F NMR allows one to determine the individual isomers, the populations, and the exchange rates between the isomers in the DOTA–Ln like tags. A paramagnetic tag with slower exchange rates between different conformations is more likely to perverse the paramagnetic behavior in its protein conjugates. Such information sets valuable guidelines in the design and evaluation of suitable paramagnetic tags for site-specific tagging proteins. This method can be extended into other paramagnetic tags containing the open-chain metal chelating moieties, since the fluorine group is readily encoded into the tags in organic synthesis steps. With increasing interests of ^{19}F NMR in structural and chemical biology,[17] we believe that suitable paramagnetic tags in combination with sensitive ^{19}F-repoter will find wide applications in this field.

This work was supported by the National Natural Science Foundation of China (21991081 and 21273121 and 21473095).

Conflicts of interest

There are no conflicts to declare.

Notes and references

1 (*a*) I. Bertini, C. Luchinat and G. Parigi, *Prog. Nucl. Magn. Reson. Spectrosc.*, 2002, **40**, 249–273; (*b*) G. Parigi, E. Ravera and C. Luchinat, *Prog. Nucl. Magn. Reson. Spectrosc.*, 2019, **114–115**, 211–236; (*c*) G. Otting, *Annu. Rev. Biophys.*, 2010, **39**, 387–405.

2 (*a*) G. Pintacuda, M. John, X.-C. Su and G. Otting, *Acc. Chem. Res.*, 2007, **40**, 206–212; (*b*) M. A. S. Hass and M. Ubbink, *Curr. Opin. Struct. Biol.*, 2014, **24**, 45–53; (*c*) Z. Wu, M. D. Lee, T. J. Carruthers, M. Szabo, M. L. Dennis, J. D. Swarbrick, B. Graham and G. Otting, *Bioconjugate Chem.*, 2017, **28**, 1741–1748; (*d*) S. Täubert, Y.-H. Zhang, M. M. Martinez, F. Siepel, E. Wöltjen, A. Leonov and C. Griesinger, *ChemBioChem*, 2020, **21**, 3333–3337; (*e*) M. Erdélyi, E. ĎAuvergne, A. Navarro-Vázquez, A. Leonov and C. Griesinger, *Chem. – Eur. J.*, 2011, **17**, 9368–9376; (*f*) A. Canales, A. Mallagaray, J. Pérez-Castells, I. Boos, C. Unverzagt, S. André, H. J. Gabius, F. J. Cañada and J. Jiménez-Barbero, *Angew. Chem., Int. Ed.*, 2013, **52**, 13789–13793.

3 (*a*) F. Rodriguez-Castañeda, P. Haberz, A. Leonov and C. Griesinger, *Magn. Reson. Chem.*, 2006, **44**, S10–S16; (*b*) J. Koehler and J. Meiler, *Prog. Nucl. Magn. Reson. Spectrosc.*, 2011, **59**, 360–389; (*c*) W.-M. Liu, M. Overland and M. Ubbink, *Coord. Chem. Rev.*, 2014, **273–274**, 2–12; (*d*) C. Nitsche and G. Otting, *Prog. Nucl. Magn. Reson. Spectrosc.*, 2017, **98–99**, 20–49; (*e*) X.-C. Su and J.-L. Chen, *Acc. Chem. Res.*, 2019, **52**, 1675–1686; (*f*) D. Joss and D. Häussinger, *Prog. Nucl. Magn. Reson. Spectrosc.*, 2019, **114–115**, 284–312; (*g*) M. Denis, C. Softley, S. Giuntini, M. Gentili, E. Ravera, G. Parigi, M. Fragai, G. Popowicz, M. Sattler, C. Luchinat, L. Cerofolini and C. Nativi, *ChemPhysChem*, 2020, **21**, 863–869.

4 (*a*) Q.-F. Li, Y. Yang, A. Maleckis, G. Otting and X.-C. Su, *Chem. Commun.*, 2012, **48**, 2704–2706; (*b*) T. Ikegami, L. Verdier, P. Sakhaii, S. Grimme, B. Pescatore, K. Saxena, K. M. Fiebig and C. Griesinger, *J. Biomol. NMR*, 2004, **29**, 339–349; (*c*) G. Pintacuda, A. Moshref, A. Leonchiks, A. Sharipo and G. Otting, *J. Biomol. NMR*, 2004, **29**, 351–361; (*d*) M. Prudêncio, J. Rohovec, J. A. Peters, E. Tocheva, M. J. Boulanger, M. E. P. Murphy, H.-J. Hupkes, W. Kosters, A. Impagliazzo and M. Ubbink, *Chem. – Eur. J.*, 2004, **10**, 3252–3260.

5 (*a*) F. Peters, M. Maestre-Martinez, A. Leonov, L. Kovačič, S. Becker, R. Boelens and C. Griesinger, *J. Biomol. NMR*, 2011, **51**, 329–337; (*b*) M. D. Vlasie, C. Comuzzi, A. M. C. H. van den Nieuwendijk, M. Prudêncio, M. Overhand and M. Ubbink, *Chem. – Eur. J.*, 2007, **13**, 1715–1723; (*c*) M. A. S. Hass, W.-M. Liu, R. V. Agafonov, R. Otten, L. A. Phung, J. T. Schilder, D. Kern and M. Ubbink, *J. Biomol. NMR*, 2015, **61**, 123–136; (*d*) D. Häussinger, J.-R. Huang and S. Grzesiek, *J. Am. Chem. Soc.*, 2009, **131**, 14761–14767; (*e*) A. C. L. Opina, M. Strickland, Y.-S. Lee, N. Tjandra, R. A. Byrd, R. E. Swenson and O. Vasalatiy, *Dalton Trans.*, 2016, **45**, 4673–4687; (*f*) J.-L. Chen, B. Li, X.-Y. Li and X.-C. Su, *J. Phys. Chem. Lett.*, 2020, **11**, 9493–9500.

6 I. Bertini and C. Luchinat, *Coord. Chem. Rev.*, 1996, **150**, 77–110.

7 (*a*) S. Aime, M. Botta and G. Ermondi, *Inorg. Chem.*, 1992, **31**, 4291–4299; (*b*) S. Hoeft and K. Roth, *Chem. Ber.*, 1993, **126**, 869–873; (*c*) M. Meyer, V. Dahaoui-Gindrey, C. Lecomte and R. Guilard, *Coord. Chem. Rev.*, 1998, **178–180**, 1313–1405.

8 (*a*) M. Woods, S. Aime, M. Botta, J. A. K. Howard, J. M. Moloney, M. Navet, D. Parker, M. Port and O. Rousseaux, *J. Am. Chem. Soc.*, 2000, **122**, 9781–9792; (*b*) F. A. Dunand, S. Aime and A. E. Merbach, *J. Am. Chem. Soc.*, 2000, **122**, 1506–1512; (*c*) V. S. Mironov, Y. G. Galyametdinov, A. Ceulemans, C. Görller-Walrand and K. Binnemans, *Chem. Phys. Lett.*, 2001, **345**, 132–140; (*d*) M. Strickland, C. D. Schwieters, C. Göbl, A. C. L. Opina, M.-P. Strub, R. E. Swenson, O. Vasalatiy and N. Tjandra, *J. Biomol. NMR*, 2016, **66**, 125–139.

9 Y. Yang, F. Yang, Y.-J. Gong, J.-L. Chen, D. Goldfarb and X.-C. Su, *Angew. Chem., Int. Ed.*, 2017, **56**, 2914–2918.

10 Y. Yang, J.-T. Wang, Y.-Y. Pei and X.-C. Su, *Chem. Commun.*, 2015, **51**, 2824–2827.

11 (*a*) S. Aime, M. Botta, D. Parker and J. G. Williams, *J. Chem. Soc., Dalton Trans.*, 1996, **2**, 17–23; (*b*) R. S. Dickins, D. Parker, J. I. Bruce and D. J. Tozer, *Dalton Trans.*, 2003, 1264–1271; (*c*) J. Kotek, J. Rudovský, P. Hermann and I. Lukeš, *Inorg. Chem.*, 2006, **45**, 3097–3102; (*d*) D. D. Castelli, M. C. Caligara, M. Botta, E. Terreno and S. Aime, *Inorg. Chem.*, 2013, **52**, 7130–7138.

12 (*a*) B. Bleaney, *J. Magn. Reson.*, 1972, **8**, 91–100; (*b*) C. N. Reilley and B. W. Good, *Anal. Chem.*, 1975, **47**, 2110–2116; (*c*) R. M. Golding and P. Halton, *Aust. J. Chem.*, 1972, **25**, 2577–2581.

13 (*a*) S. Aime, M. Botta, M. Fasano, M. P. M. Marques, C. F. G. C. Geraldes, D. Pubanz and A. E. Merbach, *Inorg. Chem.*, 1997, **36**, 2059–2068; (*b*) A. Takács, R. Napolitano, M. Purgel, A. C. Bényei, L. Zékány, E. Brücher, I. Tóth, Z. Baranyai and S. Aime, *Inorg. Chem.*, 2014, **53**, 2858–2872; (*c*) M. Woods, Z. Kovacs, R. Kiraly, E. Brücher, S. Zhang and A. D. Sherry, *Inorg. Chem.*, 2004, **43**, 2845–2851; (*d*) S. Aime, M. Botta, Z. Garda, B. E. Kucera, G. Tircso, V. G. Young and M. Woods, *Inorg. Chem.*, 2011, **50**, 7955–7965; (*e*) S. Aime, A. S. Batsanov, M. Botta, J. A. K. Howard, M. P. Lowe and D. Parker, *New J. Chem.*, 1999, **23**, 669–670.

14 (*a*) V. Jacques and J. F. Desreux, *Inorg. Chem.*, 1994, **33**, 4048–4053; (*b*) J. A. K. Howard, A. M. Kenwright, J. M. Moloney, D. Parker, M. Port, M. Navet, O. Rousseau and M. Woods, *Chem. Commun.*, 1998, 1381–1382; (*c*) L. Di Bari, G. Pintacuda and P. Salvadori, *Eur. J. Inorg. Chem.*, 2000, 75–82.

15 T. Vitha, V. Kubíček, J. Kotek, P. Hermann, L. Vander Elst, R. N. Muller, I. Lukeš and J. A. Peters, *Dalton Trans.*, 2009, 3204–3214.

16 F. Yang, X. Wang, B. B. Pan and X.-C. Su, *Chem. Commun.*, 2016, **52**, 11535–11538.

17 (*a*) E. Matei and A. M. Gronenborn, *Angew. Chem., Int. Ed.*, 2016, **55**, 150–154; (*b*) J. Gao, E. Liang, R. Ma, F. Li, Y. Liu, J. Liu, L. Jiang, C. Li, H. Dai, J. Wu, X. Su, W. He and K. Ruan, *Angew. Chem., Int. Ed.*, 2017, **56**, 12982–12986; (*c*) Y. Huang, X. Wang, G. Lv, A. M. Razavi, G. H. M. Huysmans, H. Weinstein, C. Bracken, D. Eliezer and O. Boudker, *Nat. Chem. Biol.*, 2020, **16**, 1006–1012.

